

Tuning of narrow geometric resonances in Ag/Au binary nanoparticle arrays

Jia Li, Ying Gu*, and Qihuang Gong¹

State Key Laboratory for Mesoscopic Physics and Department of Physics, Peking University,
Beijing 100871, China

¹qhong@pku.edu.cn

[*ygu@pku.edu.cn](mailto:ygu@pku.edu.cn)

Abstract: We extend the coupled dipole method to a semianalytical method that can be applied with high efficiency and accuracy to metallic heterogeneous binary particle arrays. The spectrum of the binary structure that we propose, which is composed of alternating silver and gold spherical nanoparticles, is characterized by additional geometric resonances near diffraction orders that originate from the real periodicity (i.e., twice the interparticle distance). The new diffraction orders can force the induced polarization of the heterogeneous particles out of phase, so that light scattered from them interferes destructively, which leads to geometric resonances imposed by destructive interference. By varying the constituent particle sizes, both the width and intensity of the additional geometric resonances can be effectively tuned. In particular, the Fano profiles of the geometric resonances can be tuned and are inverted when the contrast in scattering capabilities of the two types of constituent particles changes. The extensive tunability of the binary structure makes itself highly desirable for design of plasmon-based chemical and biological sensors.

© 2010 Optical Society of America

OCIS codes: (240.6680) Surface plasmons; (230.4555) Coupled resonators.

References and links

1. K. T. Carron, W. Fluhr, M. Meier, A. Wokaun, and H. W. Lehmann, "Resonances of two-dimensional particle gratings in surface-enhanced Raman scattering," *J. Opt. Soc. Am. B* **3**, 430–440 (1986).
2. S. Zou, N. Janel, and G. C. Schatz, "Silver nanoparticle array structures that produce remarkably narrow plasmon lineshapes," *J. Chem. Phys.* **120**, 10871–10875 (2004).
3. S. Zou and G. C. Schatz, "Narrow plasmonic/hotonic extinction and scattering line shapes for one and two dimensional silver nanoparticle arrays," *J. Chem. Phys.* **121**, 12606–12612 (2004).
4. V. A. Markel, "Divergence of dipole sums and the nature of non-Lorentzian exponentially narrow resonances in one-dimensional periodic arrays of nanospheres," *J. Phys. B* **38**, 115–121 (2005).
5. B. Auguie and W. L. Barnes, "Collective resonances in gold nanoparticle arrays," *Phys. Rev. Lett.* **101**, 143902 (2008).
6. V. G. Kravets, F. Schedin, and A. N. Grigorenko, "Extremely narrow plasmon resonances based on diffraction coupling of localized plasmons in arrays of metallic nanoparticles," *Phys. Rev. Lett.* **101**, 087403 (2008).
7. M. Inoue, K. Ohtaka, and S. Yanagawa, "Light scattering from macroscopic spherical bodies. 11. Reflectivity of light and electromagnetic localized state in a periodic monolayer of dielectric spheres," *Phys. Rev. B* **25**, 689–699 (1982).
8. R. G. Newton, "Optical theorem and beyond," *Am. J. Phys.* **44**, 639–642 (1976).
9. U. Fano, "Effects of configuration interaction on intensities and phase shifts," *Phys. Rev.* **124**, 1866–1878 (1961).
10. G. Bachelier, I. Russier-Antoine, E. Benichou, C. Jonin, N. Del Fatti, F. Vallee, and P.-F. Brevet, "Fano profiles induced by near-field coupling in heterogeneous dimers of gold and silver nanoparticles," *Phys. Rev. Lett.* **101**, 197401 (2008).

11. A. Christ, Y. Ekinici, H. H. Solak, N. A. Gippius, S. G. Tikhodeev, and O. J. F. Martin, "Controlling the Fano interference in a plasmonic lattice," *Phys. Rev. B* **76**, 201405 (2007).
12. S. Collin, G. Vincent, R. Haidar, N. Bardou, S. Rommeluere, and J. L. Pelouard, "Nearly perfect Fano transmission resonances through nanoslits drilled in a metallic membrane," *Phys. Rev. Lett.* **104**, 027401 (2010)
13. E. M. Purcell and C. R. Pennypacker, "Scattering and absorption of light by nonspherical dielectric grains," *Astrophys. J.* **186**, 705–714 (1973).
14. U. Laor and G. C. Schatz, "The role of surface roughness in surface enhanced raman spectroscopy (SERS): the importance of multiple plasmon resonances," *Chem. Phys. Lett.* **82**, 566–570 (1981).
15. V. A. Markel, "Coupled-dipole approach to scattering of light from a one-dimensional periodic dipole structure," *J. Mod. Opt.* **40**, 2281–2291 (1993).
16. L. Zhao, K. L. Kelly, and G. C. Schatz, "The extinction spectra of silver nanoparticle arrays: influence of array structure on plasmon resonance wavelength and width," *J. Phys. Chem. B*, **107**, 7343–7350 (2003).
17. Draine B T, "The discrete-dipole approximation and its application to interstellar graphite grains" *Astrophys. J.* **333**, 848–872 (1988).
18. D. W. Lynch and W. R. Hunter, in *Handbook of optical constants of solids*, E. D. Palik (Academic Press, New York, 1985), pp. 350.
19. A. A. Lazarides and G. C. Schatz, "DNA-linked metal nanosphere materials: structural basis for the optical properties," *J. Phys. Chem. B* **104**, 460–467 (2000).
20. S. Zou and G. C. Schatz, "Response to 'Comment on 'Silver nanoparticle array structures that produce remarkable narrow plasmon line shapes' "[*J. Chem. Phys.* 120, 10871 (2004)]" *J. Chem. Phys.* **122**, 097102 (2005).

1. Introduction

The extremely narrow geometric resonances in metallic nanoparticle arrays have attracted significant attention because of their potential use in applications that demand high quality-factor resonances, such as nanolasers, nanolenses, metamaterials and biosensors. Light is multiply scattered by the regularly spaced particles, which can lead to a geometric resonance when the wavelength of the scattered light is commensurate with the periodicity of the array. The geometric resonance can be considerably enhanced when it occurs in the same spectral range as a localized surface plasmon resonance (LSPR). In a particle array, geometric resonances are directly related to diffraction orders [1]. A strong change in the radiated intensity occurs near the critical energy where one particular diffraction order changes from radiating to evanescent. At slightly lower frequencies, the evanescent order, which means no radiation from the array, may give rise to a very sharp resonance [1]. The narrowest geometric resonances (< 1 meV) have been achieved in one dimensional silver nanoparticle arrays in which both the polarization and wave vector of the incident wave are perpendicular to the array axis [2]. The resonance line shape is remarkably robust to random array disorder [3, 4]. This narrow resonance is also produced in arrays composed of a variety of shapes such as cylindrical disks [3] and ellipsoidal particles [5], or even dimers [6].

Geometric resonances in metallic or even dielectric particle [7] arrays composed of unitary particles (which are hereafter called unitary arrays) have been extensively studied. In unitary arrays, the constructive interference of the scattered light, especially in the forward direction, is crucial for producing enhanced geometric resonances because the total extinction depends only on the forward scattering amplitude [8]. When the incident wave vector is perpendicular to the array axis, the induced polarization of every particle should be the same, so light scattered by each particle in the forward direction has the same phase and interferes constructively, which leads to enhanced resonances [2]. In this paper, we propose a type of array that is composed of alternating silver and gold particles. Because of their heterogeneity, the induced polarization of the two types of particles should be different, so various interference effects are expected. We show herein that binary nanoparticle arrays (which are also called binary arrays for brevity) present additional geometric resonances, for which the induced polarization of heterogeneous particles is out of phase so light scattered by them interferes destructively. The destructive interference offers a convenient method to control the resonance intensity and results in dramatic modifications of the Fano profiles of these additional geometric resonances.

Fano interference arises whenever scattering from an input state can occur via two distinct pathways; either directly toward a continuum of extended states or resonantly through a discrete energy level [9]. In nature, all geometric resonances exhibit Fano profiles, in which the non-resonant path is related to the direct transmission of light through arrays and the resonant path corresponds to the discrete collective plasmonic excitations along the array plane [5]. Recently, Fano interferences in plasmonic systems have attracted much attention. Fano profiles were first demonstrated in a pure plasmonic system where the LSPR of the silver nanoparticle (the discrete level) is coupled to the interband transitions of the gold nanoparticle (the continuum) because of near-field coupling in the dimer [10]. In a two-layer plasmonic lattice system, the spectral interference between super- and subradiant normal modes results in Fano profiles that are directly controlled by the spacing and alignment of the stacked lattice planes [11]. Nearly perfect Fano transmission has been demonstrated in nanoslits drilled in a metallic membrane, which has been applied to the design of high-efficiency single-layer spectral bandpass filters [12]. In unitary arrays, the Fano profiles of geometric resonances are mainly determined by geometric parameters and are difficult to control. In our binary array structures, the destructive interference in those additional resonances leads to good tunability of the Fano profiles. In particular, an inversion of the Fano profiles has been achieved.

In this paper, we first extend the coupled dipole method to a new semianalytical method, which allows us to accurately and efficiently address binary heterogeneous arrays. Compared with unitary arrays, Ag/Au binary arrays present additional geometric resonances near new diffraction orders that originate from the real periodicity that is twice the interparticle distance. A new diffraction order can polarize heterogeneous constituent particles out of phase and, consequently, light scattered by these particles interferes destructively. Because of the destructive interference, the width and intensity of a new geometric resonance can be controlled by varying the constituent particle size. The Fano profiles can also be tuned and in particular, Fano profiles are inverted because of changes in the contrast between the scattering capabilities of heterogeneous particles. This proposed binary structure is a potential candidate for use in nanophotonics devices such as plasmonic lenses and sensors.

2. Semianalytical extended coupled dipole method and retarded dipole sums

The coupled dipole (CD) method is widely used to solve problems involving nanoparticle arrays [13, 14, 15] and considers both the dipolar interactions and the finite size of particles. Generally, a set of linear equations must be solved, which is time consuming when many particles are involved. For an infinite periodic array and when the wave vector is perpendicular to the array axis, a semianalytical solution is obtained by assuming that the induced polarization is the same in each array element [16]. Under the same conditions, we extend the CD method to a binary array. The extended method can also be used to address arrays with more than two types of constituent particles.

Consider an array of N particles whose positions and polarizabilities are denoted \mathbf{r}_i and α_i , respectively. The dipole \mathbf{P}_i induced in each particle by an applied plane wave field is $\mathbf{P}_i = \alpha_i \mathbf{E}_{\text{loc},i}$ ($i = 1, 2, \dots, N$), where the local field $\mathbf{E}_{\text{loc},i}$ is the sum of the incident and retarded fields of the other $N - 1$ dipoles. For a given wavelength λ , this field is

$$\mathbf{E}_{\text{loc},i} = \mathbf{E}_{\text{inc},i} + \mathbf{E}_{\text{dipole},i} = \mathbf{E}_0 \exp(i\mathbf{k} \cdot \mathbf{r}_i) - \sum_{j=1, j \neq i}^N \mathbf{A}_{ij} \cdot \mathbf{P}_j, \quad i = 1, 2, \dots, N, \quad (1)$$

where \mathbf{E}_0 and \mathbf{k} are the amplitude and wave vector of the incident wave, respectively. In general,

elements of the dipole interaction matrix \mathbf{A} are tensors and can be expressed as

$$\mathbf{A}_{ij} \cdot \mathbf{P}_j = k^2 e^{ikr_{ij}} \frac{\mathbf{r}_{ij} \times (\mathbf{r}_{ij} \times \mathbf{P}_j)}{r_{ij}^3} + e^{ikr_{ij}} (1 - ikr_{ij}) \frac{\mathbf{r}_{ij}^2 \mathbf{P}_j - 3\mathbf{r}_{ij}(\mathbf{r}_{ij} \cdot \mathbf{P}_j)}{r_{ij}^5},$$

$$i = 1, 2, \dots, N, j = 1, 2, \dots, N, j \neq i, \quad (2)$$

where \mathbf{r}_{ij} is the vector from dipole i to dipole j . The polarization vectors are obtained by solving $3N$ linear equations of the form

$$\mathbf{A}' \mathbf{P} = \mathbf{E}, \quad (3)$$

where the off-diagonal elements \mathbf{A}'_{ij} of the matrix are the same as \mathbf{A}_{ij} , and the diagonal elements \mathbf{A}'_{ii} are α_i^{-1} (α_i is the polarizability of particle i). After obtaining the polarization vectors, we can calculate the extinction cross sections using [17]:

$$C_{\text{ext}} = \frac{4\pi k}{|\mathbf{E}_0|^2} \sum_{j=1}^N \text{Im}(\mathbf{E}_{\text{inc},j}^* \cdot \mathbf{P}_j). \quad (4)$$

In an infinite binary particle array ($N \rightarrow \infty$), when the wave vector is perpendicular to the array, the same type of particles have the same induced polarization because of spatial symmetry. The two neighboring heterogeneous particles 1 and 2 are characterized by polarizability α_1 and α_2 . Particles located at $\dots, -3d, -1d, 1d, 3d, \dots$ have the same induced polarization \mathbf{P}_1 as particle 1, and particles located at $\dots, -4d, -2d, 0d, 2d, \dots$ have the same induced polarization \mathbf{P}_2 as particle 2. Recalling Eq. (1),

$$\begin{aligned} \mathbf{E}_{\text{loc},1} &= \mathbf{E}_0 - (\dots + \mathbf{A}_{1,-3} \cdot \mathbf{P}_1 + \mathbf{A}_{1,-2} \cdot \mathbf{P}_2 + \mathbf{A}_{1,-1} \cdot \mathbf{P}_1 + \mathbf{A}_{1,0} \cdot \mathbf{P}_2 \\ &\quad + \mathbf{A}_{1,2} \cdot \mathbf{P}_2 + \mathbf{A}_{1,3} \cdot \mathbf{P}_1 + \mathbf{A}_{1,4} \cdot \mathbf{P}_2 + \mathbf{A}_{1,5} \cdot \mathbf{P}_1 + \dots), \\ \mathbf{E}_{\text{loc},2} &= \mathbf{E}_0 - (\dots + \mathbf{A}_{2,-2} \cdot \mathbf{P}_2 + \mathbf{A}_{2,-1} \cdot \mathbf{P}_1 + \mathbf{A}_{2,0} \cdot \mathbf{P}_2 + \mathbf{A}_{2,1} \cdot \mathbf{P}_1 \\ &\quad + \mathbf{A}_{2,3} \cdot \mathbf{P}_1 + \mathbf{A}_{2,4} \cdot \mathbf{P}_2 + \mathbf{A}_{2,5} \cdot \mathbf{P}_1 + \mathbf{A}_{2,6} \cdot \mathbf{P}_2 + \dots). \end{aligned} \quad (5)$$

Elements of the dipole interaction matrix depend on \mathbf{r}_{ij} . For one dimensional arrays, we can rewrite $\mathbf{A}_{2,5}$ as \mathbf{A}_{3d} , etc. Eq. (5) then becomes

$$\begin{aligned} \mathbf{E}_{\text{loc},1} &= \mathbf{E}_0 - (\dots + \mathbf{A}_{-4d} + \mathbf{A}_{-2d} + \mathbf{A}_{2d} + \mathbf{A}_{4d} + \dots) \cdot \mathbf{P}_1 \\ &\quad - (\mathbf{A}_{-3d} + \mathbf{A}_{-d} + \mathbf{A}_d + \mathbf{A}_{3d} + \dots) \cdot \mathbf{P}_2, \\ \mathbf{E}_{\text{loc},2} &= \mathbf{E}_0 - (\dots + \mathbf{A}_{-4d} + \mathbf{A}_{-2d} + \mathbf{A}_{2d} + \mathbf{A}_{4d} + \dots) \cdot \mathbf{P}_2 \\ &\quad - (\mathbf{A}_{-3d} + \mathbf{A}_{-d} + \mathbf{A}_d + \mathbf{A}_{3d} + \dots) \cdot \mathbf{P}_1. \end{aligned} \quad (6)$$

We define two partial retarded dipole sums \mathbf{S}_{odd} and \mathbf{S}_{even}

$$\begin{aligned} \mathbf{S}_{\text{odd}} &= \dots - \mathbf{A}_{-3d} - \mathbf{A}_{-d} - \mathbf{A}_d - \mathbf{A}_{3d} - \dots, \\ \mathbf{S}_{\text{even}} &= \dots - \mathbf{A}_{-4d} - \mathbf{A}_{-2d} - \mathbf{A}_{2d} - \mathbf{A}_{4d} - \dots, \end{aligned} \quad (7)$$

In periodic particle arrays, particles are polarized in the same direction as the incident wave, so the partial retarded dipole sums can be regarded just as coefficients and can be evaluated numerically using

$$\begin{aligned} S_{\text{odd}} &= \sum_{|r_{ij}|=(2n-1)d} \left[\frac{(1 - ikr_{ij}) \times (3 \cos^2 \theta_{ij} - 1) e^{ikr_{ij}}}{r_{ij}^3} + \frac{k^2 \sin^2 \theta_{ij} e^{ikr_{ij}}}{r_{ij}} \right], \\ S_{\text{even}} &= \sum_{|r_{ij}|=2nd} \left[\frac{(1 - ikr_{ij}) \times (3 \cos^2 \theta_{ij} - 1) e^{ikr_{ij}}}{r_{ij}^3} + \frac{k^2 \sin^2 \theta_{ij} e^{ikr_{ij}}}{r_{ij}} \right], \quad n = 1, 2, 3, \dots, \end{aligned} \quad (8)$$

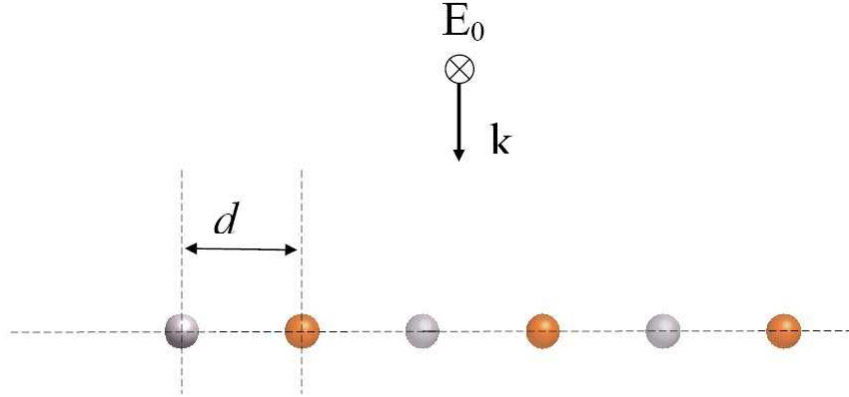


Fig. 1. Scheme of a Ag/Au binary array. Both the wave vector and polarization of the incident wave are perpendicular to the array axis.

where θ_{ij} is the angle between \mathbf{r}_{ij} and the polarization direction. The local fields at positions $1d$ and $2d$ also induce polarizations:

$$\mathbf{P}_1 = \alpha_1 \mathbf{E}_{\text{loc},1}, \quad \mathbf{P}_2 = \alpha_2 \mathbf{E}_{\text{loc},2}, \quad (9)$$

and consequently,

$$\mathbf{E}_{\text{loc},1} = \frac{\mathbf{P}_1}{\alpha_1}, \quad \mathbf{E}_{\text{loc},2} = \frac{\mathbf{P}_2}{\alpha_2}. \quad (10)$$

Using Eqs. (6), (7), and (10), we obtain

$$\frac{\mathbf{P}_1}{\alpha_1} = \mathbf{E}_0 + S_{\text{even}} \mathbf{P}_1 + S_{\text{odd}} \mathbf{P}_2, \quad \frac{\mathbf{P}_2}{\alpha_2} = \mathbf{E}_0 + S_{\text{even}} \mathbf{P}_2 + S_{\text{odd}} \mathbf{P}_1. \quad (11)$$

Solving these two equations yields

$$\begin{aligned} \mathbf{P}_1 &= \frac{1/\alpha_2 - (S_{\text{even}} - S_{\text{odd}})}{(1/\alpha_2 - S_{\text{even}})(1/\alpha_1 - S_{\text{even}}) - S_{\text{odd}}^2} \mathbf{E}_0, \\ \mathbf{P}_2 &= \frac{1/\alpha_1 - (S_{\text{even}} - S_{\text{odd}})}{(1/\alpha_2 - S_{\text{even}})(1/\alpha_1 - S_{\text{even}}) - S_{\text{odd}}^2} \mathbf{E}_0. \end{aligned} \quad (12)$$

Using the induced polarizations of each particle given in Eq. (12), the extinction cross section of the array can be deduced with the help of Eq. (4). The result is

$$C_{\text{ext}} = 2\pi N k \text{Im} \left[\frac{(1/\alpha_1 + 1/\alpha_2) - 2(S_{\text{even}} - S_{\text{odd}})}{(1/\alpha_2 - S_{\text{even}})(1/\alpha_1 - S_{\text{even}}) - S_{\text{odd}}^2} \right]. \quad (13)$$

The absorption and scattering cross sections can also be calculated from the induced polarizations [17]. For a unitary array, and assuming $\alpha_1 = \alpha_2 = \alpha$ and $S = S_{\text{even}} + S_{\text{odd}}$, the polarizations

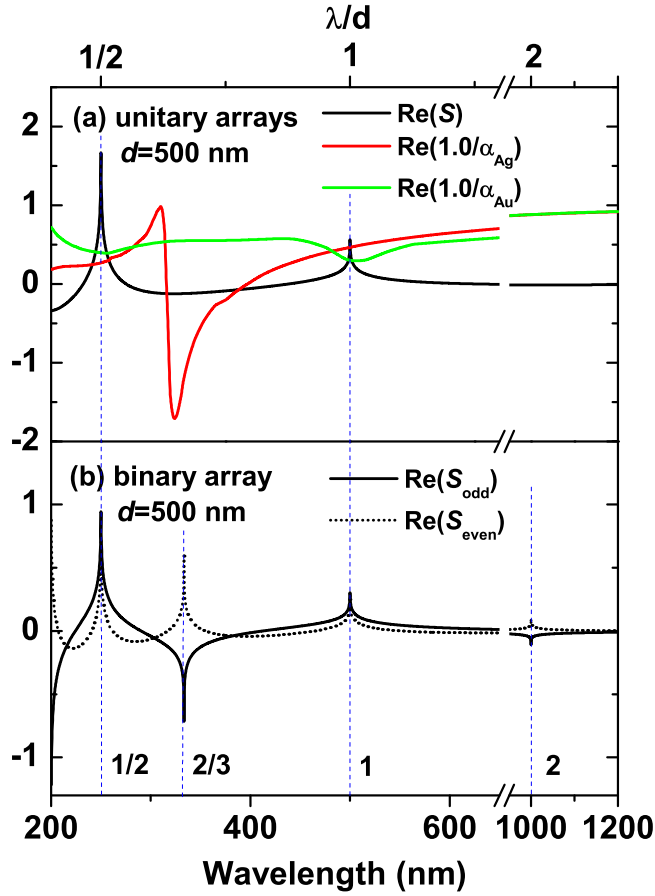


Fig. 2. (a) Real part of retarded dipole sums S of a unitary array with the interparticle distance $d = 500$ nm and the reciprocal of the dipole polarizabilities of silver and gold spheres with the radii $R=50$ nm. (b) S_{odd} and S_{even} for a binary array with the interparticle distance $d = 500$ nm. For convenience, all quantities are normalized by a factor R^3 .

in Eq. (12) and the extinction cross section of the array in Eq. (13) become

$$\mathbf{P}_1 = \mathbf{P}_2 = \mathbf{P} = \frac{\mathbf{E}_0}{1/\alpha - S}, \quad (14)$$

$$C_{\text{ext}} = 4\pi N k \text{Im}\left(\frac{1}{1/\alpha - S}\right). \quad (15)$$

which coincide with the result of the semianalytical method for unitary arrays [16]. Moreover, both the previous method and our semianalytical method assume that arrays are infinite in length, so a large number of particles should be evaluated to guarantee the accuracy of the dipole sums in Eq. (9). Zou *et al.* proved that a finite array that has 400 particles can produce narrow resonances very close to those in infinite arrays [2]. In the following calculations, generally 10,000 particles are used in each binary array, which translates to a very high accuracy.

In a unitary array, the retarded dipole sum S , which accounts for dipolar interactions of the array, plays a crucial role in producing geometric resonances [4]. As an example, in Fig. 2(a),

we plot the real part of S for a silver array and a gold array with periodic spacing $d = 500$ nm. The $\text{Re}(S)$ has sharp peaks at $\lambda = d/n$ ($n = 1, 2, \dots$), which correspond to diffraction orders (n) and may produce geometric resonances when they intersect with the reciprocal of dipole polarizabilities of metallic particles (the radius of all particles here is 50 nm) [4]. It is difficult to quantitatively analyze the situation for a binary array because we cannot define a simple retarded dipole sum. Fortunately, S_{odd} and S_{even} give us valuable information. For an arbitrary particle in a binary array, S_{odd} and S_{even} account for interactions from the different type particle located at a distance $(2n-1)d$ and the same type particle located at a distance $2nd$, respectively. As shown in Fig. 2(b), at $\lambda = d/n$, both $\text{Re}(S_{\text{odd}})$ and $\text{Re}(S_{\text{even}})$ have peaks, whereas near $\lambda = 2d/(2n-1)$, $\text{Re}(S_{\text{odd}})$ and $\text{Re}(S_{\text{even}})$ are equal in amplitude but opposite in sign.

Consider a geometric resonance that is dominated by one particular type of particle, for instance, $|P_2| \gg |P_1|$, $|S_{\text{odd}}P_2| \gg |E_0|$, and $|S_{\text{even}}P_2| \gg |E_0|$. Near $\lambda = d/n$, note that $S_{\text{even}} = S_{\text{odd}}$, so Eq. (11) can be approximated as

$$P_1 = \alpha_1 S_{\text{even}} P_2, \quad P_2 = \frac{E_0}{1/\alpha_2 - S_{\text{even}}}. \quad (16)$$

Near $\lambda = 2d/(2n-1)$, note that $S_{\text{even}} = -S_{\text{odd}}$, so equation (11) can be approximated as

$$P_1 = -\alpha_1 S_{\text{even}} P_2, \quad P_2 = \frac{E_0}{1/\alpha_2 - S_{\text{even}}}. \quad (17)$$

Using Eq. (9), we note that S_{even} is the same as $S(2d)$ for a unitary array which has a doubled interparticle distance. Therefore, on both occasions, particles dominating the resonance gain an induced polarization that is approximately the same as for their corresponding unitary array whose interparticle distance is $2d$. The other type of particles are imposed a polarization whose magnitude is proportional to P_2 and whose phase is the same as P_2 near $\lambda = d/n$ and opposite to P_2 near $\lambda = 2d/(2n-1)$. The result is that additional resonances may appear near $\lambda = 2d/(2n-1)$ in binary arrays, which corresponds to a series of new diffraction orders $[(2n-1)/2]$. For resonances near $\lambda = d/n$, the induced polarizations of both types of particles are in phase, so the scattered light interferes constructively in the forward direction. For resonances near $\lambda = 2d/(2n-1)$, the polarization of heterogeneous constituent particles are forced to be out of phase by the new diffraction orders that originate from the real periodicity of binary arrays and the scattered light interferes destructively in the forward direction. From a geometric point of view, there is only a single basic spacing d in a unitary array, so resonances may appear near $\lambda = d/n$. However, in a binary array, in addition to the smallest spacing d , the periodicity is $2d$ due to the heterogeneity of neighboring particles. This real periodicity reflects a new basic spacing so resonances may appear near $\lambda = 2d/n$, which include $\lambda = d/n$ and $\lambda = 2d/(2n-1)$.

The condition $|P_2| \gg |P_1|$ for Eqs. (16) and (17) means a difference in the capability to obtain the polarization. This capability is directly related to the scattering capability since the power scattered (or radiated) by an oscillating dipole is proportional to $|P|^2$ which is determined by the polarizability [17]. In the following, we will use the term scattering capability to describe the strength of a particle to scatter (or radiate) light power. From Eqs. (16) and (17), as long as there is a large difference in the scattering capabilities of the two types of particles (which means $|\alpha_2| \gg |\alpha_1|$), we can conclude that $P_1/P_2 = \alpha_1 S_{\text{even}}$ or $-\alpha_1 S_{\text{even}}$ which are independent of the phase of the α_2 . Therefore, the resonance is determined by the relative magnitude of the polarizabilities of the two types of particles and the relative phase plays a minor role.

3. Geometric resonances in Ag/Au binary nanoparticle arrays

In the following, we use silver and gold particles as constituent units of binary arrays, as shown schematically in Fig. 1. The arrays are all immersed in a vacuum (Both the plasmonic resonances and geometric resonances discussed in this paper will be redshifted if one takes into

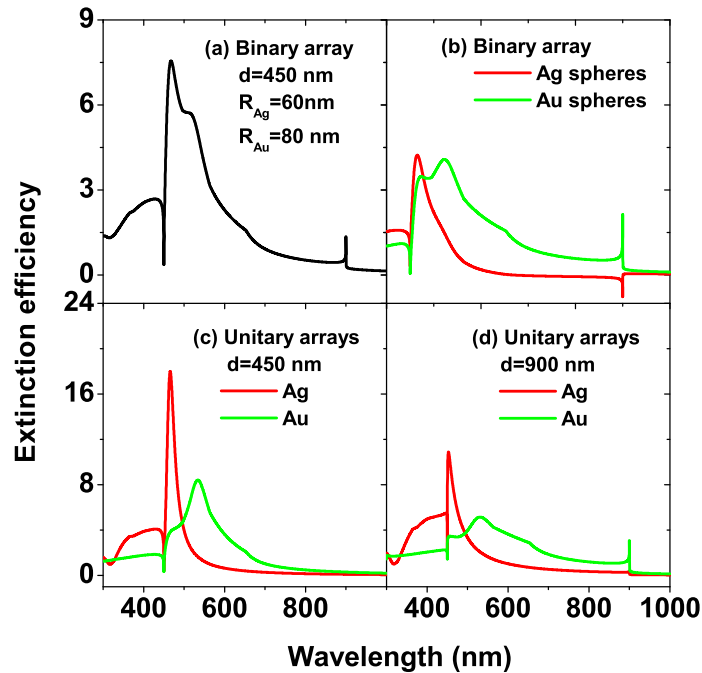


Fig. 3. (a) Extinction spectrum of a Ag/Au binary array with $d = 450$ nm interparticle distance. (b) Contributions of silver and gold constituent particles to the extinction spectrum. The corresponding unitary arrays with (c) $d = 450$ nm and (d) $d = 900$ nm. The radii of the silver and gold particles are $R_{Ag} = 60$ nm and $R_{Au} = 80$ nm, respectively.

account a surrounding medium $\epsilon_0 > 1$). The dielectric permittivities of both metals are taken from Palik [18] and the sphere polarizabilities are derived from the a_1 term of Mie theory [19]. Extinction cross sections are normalized by the geometrical area of the array. We begin the discussion of geometric resonances in a binary array by considering Fig. 3. Here, radii of silver and gold particles are $R_{Ag} = 60$ nm and $R_{Au} = 80$ nm and the wavelengths of their LSPRs are $\lambda = 430$ nm and $\lambda = 545$ nm, respectively. The interparticle distance $d = 450$ nm. The spectra of the corresponding silver and gold unitary arrays with $d = 450$ and 900 nm are also included for comparison. For the binary array whose extinction efficiency is shown in Fig. 3(a), the main geometric resonance is near $\lambda = 450$ nm and the most obvious difference from its corresponding unitary arrays with the same interparticle distance is the existence of a weaker, narrower resonance near $\lambda = 900$ nm [see Fig. 3(c)]. This is a new geometric resonance corresponding to the diffraction order (1/2), which originates from the heterogeneity of the array. Next, we use the induced polarizations of silver and gold particles to calculate their respective contributions to the extinction cross section and the result is shown in Fig. 3(b). Actually, in binary arrays, particles are coupled with each other and it is impossible to determine the exact contribution of either type of particles. However, we split the overall extinction into two parts artificially because it is very helpful for us to understand this binary structure and design specific arrays to meet our needs, which will be shown further in the following. As shown in Fig. 3(b), for the resonance near $\lambda = 450$ nm, both silver and gold particles give a positive contribution to the resonance. For the resonance near $\lambda = 900$ nm, gold particles contribute positively and silver

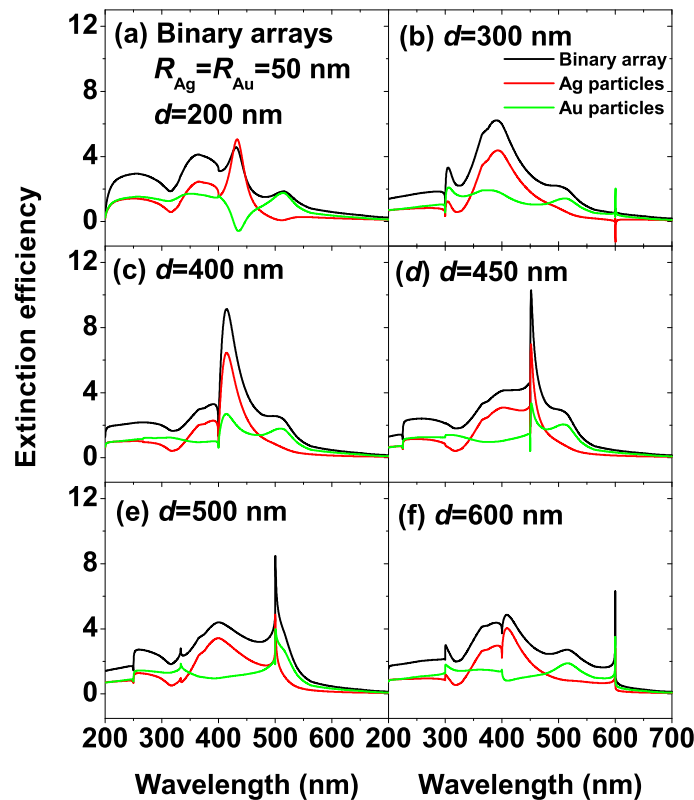


Fig. 4. Extinction spectra of Ag/Au binary arrays, in which the interparticle distance varies from (a) $d = 200$ to (f) $d = 600$ nm. The radii of all particles are $R = 50$ nm. Red (green) lines represent contributions of silver (gold) particles in arrays.

particles contribute negatively. Here, gold particles have a larger scattering capability because their LSPR peak is nearer to $\lambda = 900$ nm, so more plasmons can be excited on the surfaces of gold particles. The light scattered from gold particles forces the induced dipoles of silver particles out of phase because their spacing is about half of the resonance wavelength. Consequently, the scattering amplitude of silver particles in the forward direction and its contribution to the extinction of the arrays become negative. Thus, a negative contribution to extinction cross section just means that the scattered light of the two types of particles are out of phase. In addition, although both resonances can be observed in unitary arrays with $d = 900$ nm, only one resonance is significantly enhanced in either array, as shown in Fig. 3(d). Therefore, in a binary array, enhanced geometric resonances can be produced over a wide spectral range because of the collective contributions of the LSPRs of the constituent nanoparticles. In particular, comparing with unitary arrays with the same interparticle distance, new geometric resonances appear and the induced polarizations of the two types of constituent particles can be out of phase, resulting in geometric resonances imposed by destructive interference in binary arrays.

To further our understanding of binary arrays, we study a set of binary arrays with different

interparticle distances. In Fig. 4, we show extinction spectra of binary arrays with interparticle distances that vary from $d = 200$ to $d = 600$ nm. Here, the radii of silver and gold particles are set to $R_{\text{Ag}} = R_{\text{Au}} = 50$ nm and the wavelengths of their LSPRs is $\lambda = 405$ and 515 nm, respectively. The contributions of silver and gold nanoparticles are also included in this figure. When $d = 200$ nm, no resonance near d is observed when the diffraction order is far from the LSPRs of both the silver and gold nanoparticles. When $d = 300$ nm, the resonance near $\lambda = 300$ nm exhibits an apparent Fano profile [9], although the resonance is weak because of strong absorption by both metals. When d is increased and falls within the range of the LSPRs of the silver and gold nanoparticles, more intense geometric resonances are produced near the diffraction order (1). The LSPRs of the particles seem to be narrowed and enhanced as they merge with geometric resonances such as $d = 400$ and 500 nm. An extremely narrow geometric resonance is obtained when $d = 600$ nm because the diffraction order (1) is on the long-wavelength wing of LSPRs of both types of metallic particles. In binary particle arrays, for geometric resonances corresponding to the diffraction order (1), the LSPR spectra of both particle types form a wide joint-spectral background, which is accessible to geometric resonances.

Furthermore, new resonances corresponding to the diffraction order (1/2) appear at $\lambda = 431$ nm when $d = 200$ nm and near $\lambda = 600$ nm when $d = 300$ nm. The contribution of gold particles around $\lambda = 431$ nm is negative because it is nearer for the LSPR of silver particles exerting influences around this range than that of gold particles. Around $\lambda = 600$ nm when $d = 300$ nm, the contribution of gold particles becomes positive for similar reasons. We note that the resonance near $\lambda = 600$ nm is suppressed because of destructive interference of light scattered by heterogeneous particles. Moreover, contributions from both silver and gold particles may be positive for weak geometric resonances, such as the spikes near $\lambda = 333$ and 400 nm corresponding to the diffraction order (3/2) in Fig. 4(e) and 4(f), respectively. In these spectral regions, resonances are dominated by absorptions, which means that few plasmons can be excited and the dipolar coupling is weak. Additionally, the spikes near $\lambda = 250$ nm in Fig. 4(e) and $\lambda = 300$ nm in Fig. 4(f) correspond to the diffraction order (2). Therefore, in contrast to unitary arrays, the induced polarization of constituent particles in binary arrays is dramatically influenced by their scattering capability, which are determined by the incident wavelength and attributes of the particles such as shape, size, and dielectric permittivity.

4. Tuning widths and intensities of the geometric resonances in Ag/Au binary nanoparticle arrays

As for the new resonances that arise in binary arrays, light scattered by heterogeneous particles can interfere destructively. This characteristic can be used to directly control the intensities of these resonances. In Fig. 5(a), we show the extinction spectra of a set of binary arrays, in which the silver-particle radius varies from $R_{\text{Ag}} = 30$ to 70 nm, whereas the gold-particle radius is fixed at $R_{\text{Au}} = 70$ nm. The resonance intensity can be tuned from more than twice that of the LSPR of metallic particles to almost zero. Note that, during this tuning process, the resonance width remains essentially the same. As long as the gold-particle-scattering capability is larger than that of the silver particles around $\lambda = 600$ nm, the width of the resonance will be mainly determined by the gold-particle size. From another perspective, we can control the width of the resonance by varying the gold-particle size. In Fig. 5(b), the resonance width is continually tuned from several nm to about one hundred nm by varying the gold-particle radius from $R_{\text{Au}} = 60$ to 100 nm while maintaining the silver-particle radius at $R_{\text{Ag}} = 40$ nm. Note also that, during this tuning process, the resonance intensity remains the same almost.

The dramatic change of the resonance width results from the redshifts of the LSPR of gold particles with the gold-particle radius increasing. Here, gold particles are much larger than silver particles in size and the LSPR of gold particles is nearer to the diffraction order, so the

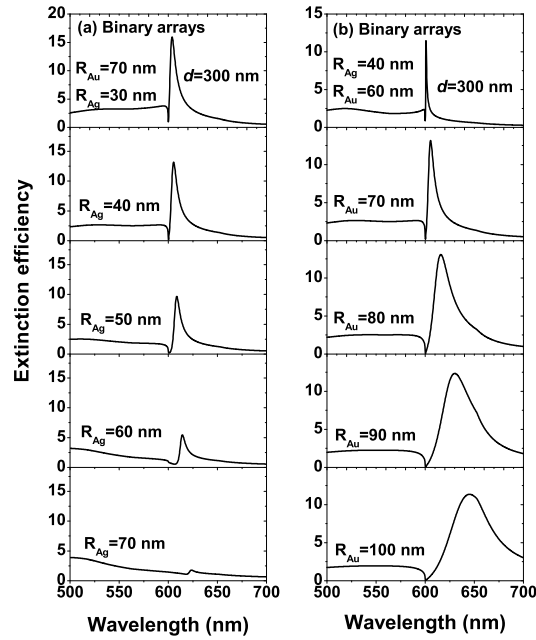


Fig. 5. Extinction spectra of Ag/Au binary arrays. In panel (a), the silver-particle radius varies from $R_{Ag} = 30$ to 70 nm while the gold-particle radius is fixed at $R_{Au} = 70$ nm. In panel (b), the gold-particle radius varies from $R_{Au} = 60$ to 100 nm while the silver-particle radius is fixed at $R_{Ag} = 40$ nm. The interparticle distance is $d = 300$ nm.

resonance is dominated by gold particles. When the diffraction order is on the long-wavelength wing of the LSPR, extremely narrow geometric resonances are obtained and their widths are determined by the geometric factors (directly related to the logarithmic singularity of the real part of the dipole sum at the diffraction order) and the imaginary part of the dipole sum plays a minor role. In this case, the width decreases when peak positions further from the LSPR. On the contrary, when the diffraction order is on the short-wavelength wing of the LSPR, the geometric and plasmonic resonances are mixed together and generally the extremely narrow geometric resonance cannot be obtained [4, 20]. Here, the gold-particle radius varies from $R_{Au} = 60$ to 100 nm. The corresponding LSPR wavelength varies from $\lambda = 521$ to 645 nm. The diffraction order at $\lambda = 600$ nm sweeps from the long-wavelength wing to the short-wavelength wing of the LSPR of gold particles, so the resonance width changes dramatically through the process. Therefore, both the width and intensity of a geometric resonance can be effectively controlled in the binary structure.

5. Tuning Fano profiles of the geometric resonances in Ag/Au binary nanoparticle arrays

In a unitary array, when a diffraction order is on the short-wavelength wing of the LSPR of the metallic particles, then the geometric resonance is broad and exhibits an obvious Fano profile [5]. When the diffraction order is on the long-wavelength wing of the LSPR, an extremely narrow and enhanced geometric resonance is obtained, and the Fano shape is concealed. However,

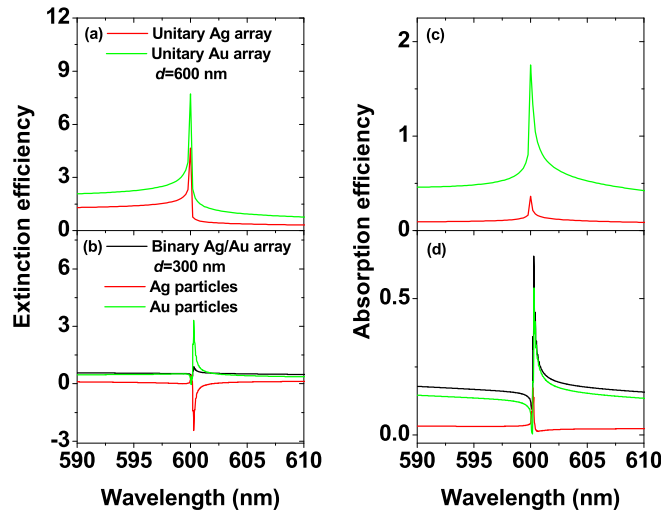


Fig. 6. Extinction spectra of (a) a silver array (red), a gold array (green), and (b) a Ag/Au binary array (black), and contributions of silver (red) and gold (green) particles. The interparticle distance is $d = 600$ nm for the unitary arrays and $d = 300$ nm for the binary array. The radii of all particles are $R = 50$ nm. Panels (c) and (d) show the corresponding absorption spectra.

in a binary array, the dipolar coupling between heterogeneous particles could induce out-of-phase polarizations, which results in a much different resonance profile in comparison with unitary arrays. In this section, we focus on Fano profiles of new geometric resonances in binary arrays and show how they can be tuned just by varying the size of the constituent particles.

We study a binary array with $R_{\text{Ag}} = R_{\text{Au}} = 50$ nm and $d = 300$ nm. The extinction spectra of silver and gold unitary arrays with $R_{\text{Ag}} = R_{\text{Au}} = 50$ nm and $d = 600$ nm are included in Fig. 6(a) for comparison. The geometric resonances near $\lambda = 600$ nm in silver and gold unitary arrays are narrow and intense, and their Fano profiles are concealed because of their extremely narrow widths. In the binary array, the corresponding resonance exhibits an apparent Fano profile, although it is rather weak because of destructive interference, as shown in Fig. 6(b). In particular, the spectra of silver and gold particles in the binary array exhibit inverse Fano profiles. Similar phenomena are observed in the corresponding absorption spectra, which are shown in Figs. 6(c) and 6(d). In what follows, we use absorption spectra to represent resonance profiles because absorption is always positive, making it convenient for the study of Fano profiles. Fig. 6(b) and 6(d) show that, when the diffraction order is on the long-wavelength wing of the LSPR, gold particles with a larger scattering capability exhibit a Fano profile similar in some degree to that for a unitary array [5]. However, silver particles have a smaller scattering capability and exhibit an abnormal Fano profile, which cannot be observed in unitary arrays.

We showed in Fig. 6 that silver and gold particles exhibit inverse Fano profiles, which is determined by their scattering capabilities. Next, we demonstrate that the Fano profiles of the new geometric resonances that appear in binary arrays can be tuned by varying the size of the constituent particles, and that an inversion of Fano profiles happens when the contrast of scattering capabilities changes. In Fig. 7, the radius of silver particles varies from $R_{\text{Ag}} = 45$ to 65 nm in 5-nm steps while the radius of gold particles is fixed at $R_{\text{Au}} = 50$ nm, and the interparticle distance $d = 300$ nm. This figure shows the absorption spectra of the binary ar-

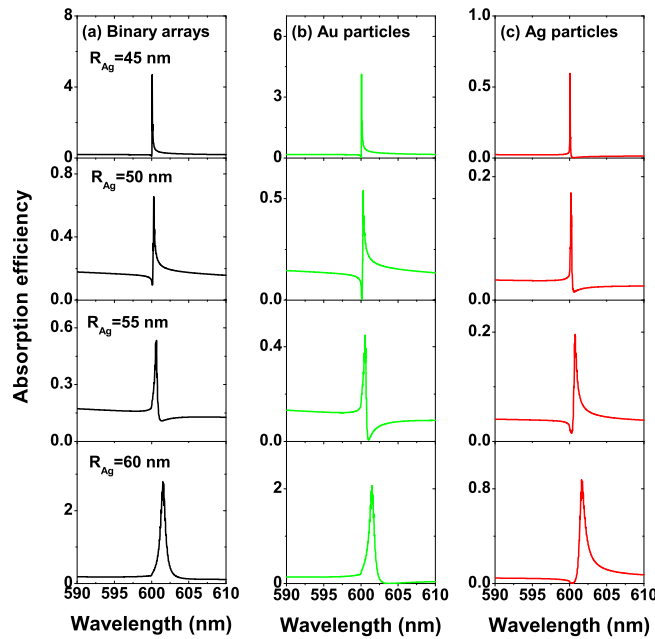


Fig. 7. (a) Absorption spectra of an Ag/Au binary array with $R_{Au} = 50$ nm and for R_{Ag} varying from 45 to 60 nm in 5-nm steps. Panels (b) and (c) show the contributions of gold and silver nanoparticles in the binary array. The interparticle distance is $d = 300$ nm.

rays and the contributions of the gold and silver constituent particles. When the silver-particle radius is small (from $R_{Ag} = 45$ to 50 nm), silver particles have a smaller scattering capability in comparison with gold particles. Thus, gold particles dominate the resonance and show normal Fano profiles, whereas silver particles show abnormal Fano profiles. At the same time, the overall resonance intensity decreases with increasing R_{Ag} because of increasing destructive interferences, as shown in Fig. 7(a). When the silver-particle radius increases to $R_{Ag} = 55$ nm, the Fano profiles are abruptly inverted. Because silver particles are now large enough to have a larger scattering capability, the polarization of the gold particle is forced out of phase and their absorption spectra exhibit abnormal Fano profiles. Correspondingly, the Fano profile of the silver particles becomes normal. During this process, the Fano profile of the array shown in Fig. 7(a) is also inverted. Similar phenomena are also observed when the gold-particle radius varies from $R_{Au} = 40$ to 70 nm while the silver-particle radius is fixed at $R_{Ag} = 50$ nm. Thus, in binary arrays, Fano profiles of new geometric resonances can be effectively tuned by varying the size of the constituent particles, and the Fano profiles may be inverted.

Finally, we briefly discuss the effect of finite length in binary arrays, which also validates our theoretical study. Both the previous calculations [16] and our semianalytical calculations are based on the hypothesis of an infinite array, which is impossible to reproduce experimentally. Zou *et al.* have shown that finite unitary arrays with 400 particles produce narrow resonances very close to those in infinite arrays [2]. We calculate the extinction efficiencies of arrays with sphere numbers varying from $N = 2$ to 150. For this calculation, we set the radii of silver and gold particles to $R_{Ag} = 30$ nm and $R_{Au} = 55$ nm, and the interparticle distance is $d = 450$

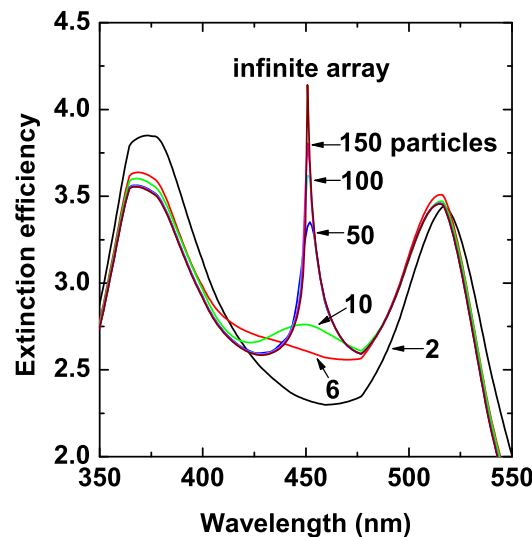


Fig. 8. Extinction spectra of finite Ag/Au binary arrays composed of different numbers of particles with the silver-particle radius $R_{\text{Ag}} = 30$ nm, the gold-particle radius $R_{\text{Au}} = 55$ nm, and the interparticle distance $d = 450$ nm.

nm. For finite arrays, we use the original CD method in which N linear equations are solved. Additionally, we use our semianalytical method to calculate an array composed of $N = 10000$ particles, which can be regarded as an infinite array. As shown in Fig. 8, when $N = 2$ or 6, only the LSPRs of silver and gold particles appear in the spectra. A geometric resonance at about $\lambda = 450$ nm starts to appear for $N = 10$, and it continues to increase in intensity and narrow in width with increasing N . When $N = 150$, both the intensity and width are very close to those expected of an infinite array. Therefore, although the present theoretical study deals with nearly infinite arrays, our result can serve as a guide for finite arrays in experimental setups.

6. Summary

Using an extended semianalytical coupled dipole method, we have studied binary arrays composed of alternating silver and gold spherical nanoparticles. In comparison with a unitary array, geometric resonances can be produced in the binary array over a wider spectral range because of the collective contributions in the binary array of the LSPRs of the silver and gold particles. Additional geometric resonances appear near new diffraction orders that originate from the heterogeneity of the binary array. These new diffraction orders force polarizations of heterogeneous particles out of phase, so that light scattered by them interferes destructively. Due to this destructive interference, both the intensities and widths of geometric resonances can be controlled. Fano profiles can be effectively tuned by varying the sizes of the constituent particles, and in particular the Fano profiles are inverted when the contrast of scattering capabilities between the two types of constituent particles changes. Although we mainly discuss in this paper binary arrays composed of silver and gold nanoparticles, most of our results are valid for other binary arrays whose constituent particles have different sizes, shapes and materials. Our theoretical study should therefore be of significant aid for making plasmon-based chemical and biological sensors.

Acknowledgments

Discussions with Prof. Xiaoyong Hu are gratefully acknowledged. This work was supported by the National Natural Science Foundation of China under Grants Nos. 10874004 and 10821062, and by the National Key Basic Research Program No. 2007CB307001.